Pergamon

Int. J. Heat Mass Transfer. Vol. 41, Nos 4–5, pp. 735–744, 1998

Printed in Great Britain
0017-9310/98 $19.00+0.00

PII: S0017-9310(97)00163-4

Vacuum assisted drying of hydrophilic plates: static drying experiments

S. W. MONTGOMERY, V. W. GOLDSCHMIDT and M. A. FRANCHEK

Ray W. Herrick Laboratories, School of Mechanical Engineering, Purdue University, West Lafayette, IN 47907-1077, U.S.A.

(*Received* 2 *December* 1996 *and in final form* 28 *May* 1997)

Abstract—This investigation seeks to identify the effects of partial vacuums on the steady-state drying rate of cotton plates. Five pressure levels between atmospheric pressure and 33.6 kPa (20″ Hg vacuum) were tested in an aluminum vacuum chamber. Improvements in steady state drying rates on the order of 62% were observed at the lowest pressure level. The hoped-for design points were not discovered. Both theoretical and experimental values of the mass transfer rate are developed. © 1997 Elsevier Science Ltd.

INTRODUCTION

The process of drying and dewatering solids is extremely energy intensive. When the solids undergoing the drying process are capable of forming powerful bonds on the molecular level with the wetting fluid, even more energy is required to effectively de-water the fluid–solid matrix [1]. Consequently, researchers have for years explored new techniques for liquid removal from solids.

One such drying technology, though hardly new, is vacuum-assisted drying. Most fluids possess a thermophysical property such that a decrease in pressure reduces the saturation temperature. In addition, the ability of the escaping fluid to diffuse through the boundary layer of air is increased due to the lower concentrations of air molecules near the surface.

The purpose of this study is to investigate drying to utilize the benefits of partial vacuums, which lead to lower drying times. Several experiments were conducted on cotton plates at various pressure levels to alter the steady state drying rates, in the hopes of achieving a point of diminishing returns. If this were indeed the case, it would then be unnecessary to construct a vacuum chamber capable of achieving high vacuums when a somewhat lower vacuum would produce the same drying rate. The lower vacuum chamber would theoretically require less maintenance due to the reduced sealing and leak-proofing requirements, as well as have a smaller initial cost.

BACKGROUND

Since the late 1920s when the first Minton dryers were used in paper production facilities, industry has recognized the benefits of partial vacuums for drying [2]. Unfortunately, the early dryers were difficult to seal, expensive and required constant maintenance, leading to a diminished use of Minton dryers. The 1970s saw a renewed interest in vacuum technology as engineers tried to increase drying rates by avoiding extra resistance to mass transfer due to the surrounding air. As a result, vacuum drying has made a partial comeback and is now receiving close scrutiny. For years, paper, heat sensitive hazardous waste, and lumber have been dried with vacuum techniques [3–5]. The key benefits of vacuum drying include lower process temperatures, less energy usage and hence greater energy efficiency, improved drying rates, and in some cases, less shrinkage of the product. Some of the recent investigations of vacuum drying are summarized in Table 1.

Åström [2] revealed the overall benefits of vacuum in a drying process. The main effect of introducing lower pressures inside a drying chamber is the pressure dependence of the boiling point of water. At atmospheric pressure, 101.325 kPa, this temperature is 100°C, while at 31.2 kPa the boiling temperature drops to 70°C. Owing to these lower temperatures, processes that relied on conduction heat transfer were improved due to the larger driving force (or, as in this case, a larger temperature gradient). Lower temperatures lead to less waste heat since the product exits the dryer at a lower temperature than it normally would without a vacuum. Åström also postulated that because of the lower required temperatures, it may be possible to utilize the waste energy from some other process to provide the energy needed for drying. Greater efficiency may also be attained by allowing the evolved water vapor to condense inside the dryer thereby minimizing the pumping capacity for the process.

Lehtinen [3] designed a piston-type vacuum dryer for flat sheets of paper, board and other permeable mats. According to the author, another benefit of vacuum drying occurs on the molecular scale, specifically, the escaping water molecules are less likely to

NOMENCLATURE

a	Luikov's diffusivity coefficient [$m^2 s^{-1}$]
C	constant
c_p	constant-pressure specific heat [$J kg^{-1} K^{-1}$]
$\dot{E}_{gen}$	rate of energy generation [W]
$\dot{E}_{in}$	rate of energy inflow [W]
$\dot{E}_{out}$	rate of energy outflow [W]
$\dot{E}_{sr}$	energy storage rate [W]
h_f	enthalpy, liquid [$J kg^{-1}$]
h_g	enthalpy, vapor [$J kg^{-1}$]
h_m	convective mass transfer coefficient [$m s^{-1}$]
h_q	convective heat transfer coefficient [$m s^{-1}$]
h_{fg}	heat of vaporization [$J kg^{-1}$]
m^*	dimensionless mass
$\dot{m}''$	rate of mass flux
p	pressure [Pa]
q	heat flow [W]
R	universal gas constant [$J kg^{-1} K^{-1}$]
t	time [s]
t^*	dimensionless time
T	temperature [K, °C, °F]
V	voltage, volume [V, m^3]
x	length coordinate [m]
y	length coordinate [m]
z	length coordinate [m].

Greek symbols

α	absorptivity
ε	emissivity
ϕ	relative humidity
ρ	density [$kg m^{-3}$].

Subscripts

∞	ambient or free stream conditions
0	initial value
evap	evaporative transfer
f	liquid state
final	final
free conv	free convection
g	vapor phase
rad	radiation
s	surface
sat	saturated.

collide with ambient gas molecules which reenter the liquid surface of the product during drying. Ahrens and Jorneaux [4] extended Lehtinen's work with an experimental apparatus and a mathematical model. The drying rates from their experimental apparatus were compared to a similar but conventional type dryer and found to have a 70% improvement. Ahrens and Jorneaux also developed a theoretical model of the dryer and matched its trends against experimental data. Forthuber and McCarty [5] developed a new drying system for heat sensitive and hazardous materials. This vacuum dryer was 47% faster than a conventional dryer operating at the same temperature. For the conventional apparatus to match the drying times achieved by their system, a 40% higher temperature was required.

Smol'skiy *et al.* [6] noted that in freeze drying under vacuum, 70% of the total energy expended is used as sublimation energy of the ice. Adding some sort of absorbent to the sample being dried also improved the drying performance.

Harris and Taras [7] performed a comprehensive comparison between standard kiln drying of wood versus a radio frequency vacuum dryer. Several performance characteristics of both process types were evaluated, including moisture content distribution and shrinkage. These tests were biased toward the conventional kiln but the vacuum chamber dried the samples in approximately 1/17th the time required for the conventional kiln. The total shrinkage for the vacuum dried sample was approximately 30% less than that of the conventional kiln. Simpson [8] performed similar tests and observed a 68% improvement in speed over a conventional kiln.

Malczewski and Kaczmarek [9] dried seeds with a vacuum process and compared their results to a convective dryer. These tests showed a 30% improvement in energy efficiency. Wadsworth *et al.* [10] examined the effects of varying chamber pressure and microwave energy for drying of rice. Their results indicated that higher levels of microwave power had less energy losses due to shorter drying times. The lower pressures also increased the drying rates.

Shi and Maupoey [11] researched water movement in fruits under vacuum and reported lower temperatures than at higher pressures, resulting in less damage to the product. Some of the test were run under a 'pulse vacuum', where the chamber was operated under vacuum for a time and then allowed to repressurize.

EXPERIMENTAL SETUP

A schematic of the vacuum test chamber is shown in Fig. 1. The vacuum chamber was constructed using 2.54 cm (1″) thick aluminum for the bottom and sides and 1.27 cm (0.5″) Lexan for the top. Analog signals are passed through four signal ports located on both sides of the chamber. A 746 W (1 HP) vacuum pump was used with the pressure relief valve to control the

Table 1. Vacuum drying literature

Author	Title	Remarks	Conclusions	Equations
Åström [2]	"The influence of vacuum on the drying of paper"	Discusses benefits of including vacuum in paper drying. Reports drying rates 10 times higher for vacuum drying than conventional methods. Quality of paper increased.	Drying occurs at lower temperatures with the use of vacuum. Waste heat minimized due to lower exit temperatures. Drying rate increases due to the shorter time needed to reach evaporation temperature.	NA
Lehtinen [3]	"A new vacuum drying method for paper, board and other permeable mats"	Piston-type apparatus presses paper into heater. Mainly a design for a proposed commercial dryer.	In vacuum drying rewetting is less likely due to fewer molecular collisions. Using a cool side increases the heat flux into the paper.	NA
Ahrens and Journeaux [4]	"An experimental and analytical investigation of a thermally induced vacuum drying process for permeable mats"	Focuses on paper drying, using a process called 'thermal/vacuum'.	Experimental data shows increased drying rates under vacuum. Interesting experimental apparatus. Constant rate period not present.	$\epsilon\rho_f\frac{\partial h_f}{\partial t} = -\frac{\partial}{\partial y}(\rho_f V_f + \rho_g V_g) + (\epsilon h_f c_{p,f}\rho_f + \epsilon(1-h_f)\rho_g c_{p,v} + (1-\epsilon)\rho_s c_{p,s})\frac{\partial T}{\partial t} + (\rho_f c_{p,f} V_f + \rho_g c_{p,g} V_g)\frac{\partial T}{\partial y} = -\frac{\partial q}{\partial y} - h_{fg}\frac{\partial}{\partial y}(\rho_g V_g)$
Forthuber and McCarty [5]	"Drying heat sensitive and/or hazardous materials utilizing a fully continuous vacuum system"	Vacuum-conductive drying eliminates some problems associated with convective drying.	Thermal degradation not present due to lower operating temperatures. More precise temperature control possible.	NA
Smol'skiy *et al.* [6]	"Heat and mass transfer through an adsorbing layer in vacuum drying of heat sensitive materials"	Looks at improving drying rates by adding an absorbent and improving the heat transfer to the phase transition surface.	Improvements are possible.	NA
Harris and Taras [7]	"Comparison of moisture content distribution, stress distribution, and shrinkage of red oak lumber dried by a radio-frequency/vacuum drying process and a conventional kiln"	Compares a number of factors involved in wood drying in a vacuum dryer vs a conventional kiln. Vacuum test slowed due to sample removal every 8 h. Conventional kiln started with lower (by 10%) moisture content.	Drying time in vacuum was 1/17th the time in the conventional kiln. Stress and moisture distributions about the same for both processes. Shrinkage was 30% less during the vacuum process than in the conventional process.	NA

Table 1—*Continued.*

Author	Title	Remarks	Conclusions	Equations
Simpson [8]	"Vacuum drying northern red oak"	Water may be evaporated at lower temperatures at the same rate it would at 212°F without the side effects associated with high temps.	Drying time not optimized. Study demonstrated good quality and shorter drying times no matter what the vacuum level.	NA
Malczewski and Kaczmarek [9]	"Vacuum contact drying of seeds"	Designed a dryer for farm use that would dry seeds quickly without loss of quality.	Vacuum contact drying more efficient than convective drying. Good agreement between experimental and theoretical curves.	$q_0'' = h_q(T_s - T)$ $q''(z,t) = q_0 \exp(-\xi^2)$ $\xi = \frac{z}{2\sqrt{a_{bed}t}}$
Wadsworth *et al.* [10]	"Microwave-vacuum drying of parboiled rice"	Study looked at the effects of varying parameters on the drying of rice.	At lower pressures drying rate and efficiency increased and rice temperature decreased. Statistical analysis performed on experimental data. Mechanism for convective drying and MW drying different.	NA
Shi and Paupoey [11]	"Vacuum osmotic dehydration of fruits"	Study to determine the effect of vacuum on water movement in fruits. Three different pressure conditions were used.	Vacuum sped up the water movement. Lower temperatures possible, maintaining high quality. Not much difference in drying between complete vacuum and pulse vacuum, but pulse vacuum used less energy.	NA

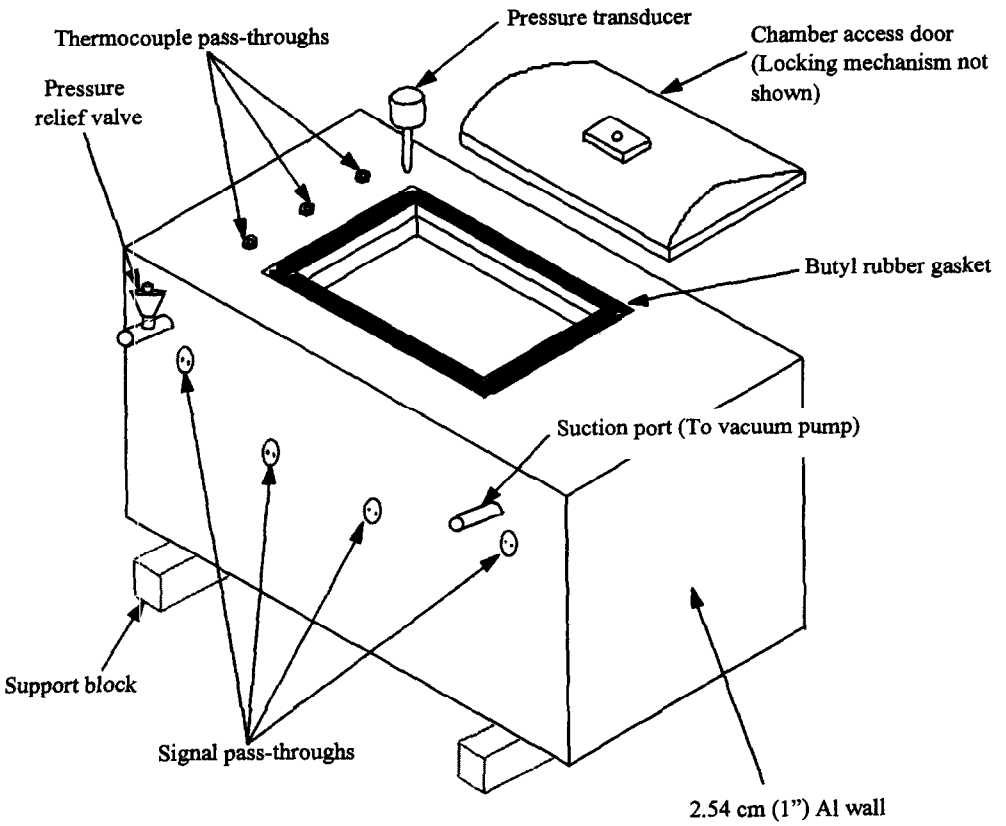

Fig. 1. Schematic of vacuum chamber.

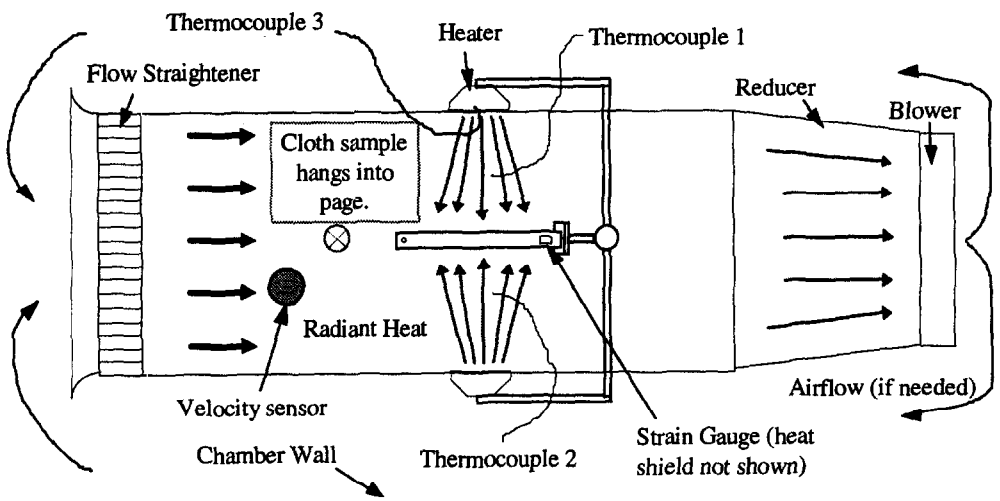

Fig. 2. Layout of dryer section (top view) within chamber.

air pressure within the chamber. The lowest internal pressure of the vacuum chamber is 30.14 kPa.

The drying section of the chamber consists of an apparatus resembling a wind tunnel which also allows for 'convective' tests. Figure 2 provides a schematic of the dryer section. Two Chromalox 800 W heaters, connected to a variable voltage source, supply radiant heat. The heaters supply an even heat distribution over the entire cloth surface (Fig. 3). The radiation view factor from the heater to the cloth surface was assumed to be unity. Two strain gauges bonded to a thin aluminum beam created the weight measurement system for the test specimen (Fig. 4).

The air pressure inside the vacuum chamber is

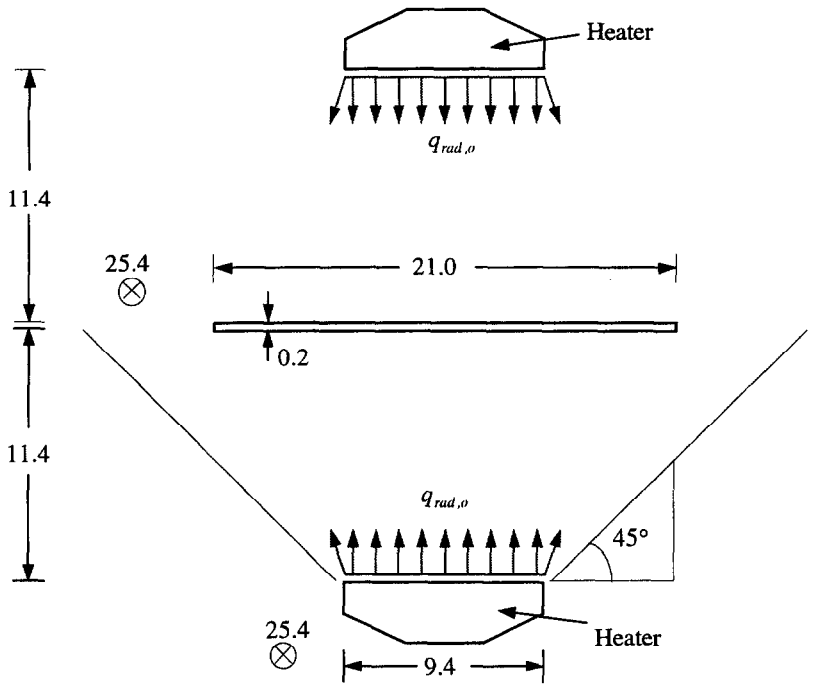

Fig. 3. Heater and cloth sample orientation (dimensions in centimeters—not to scale).

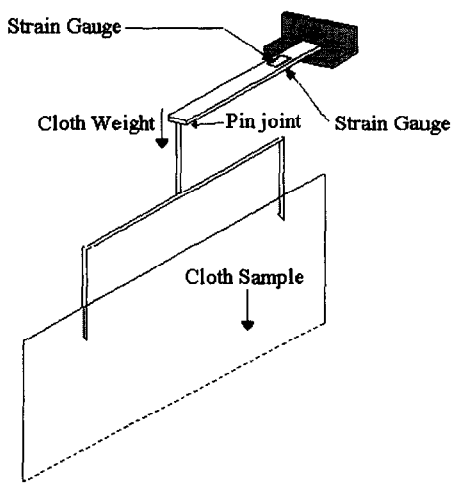

Fig. 4. Mass measurement apparatus.

evaluated three ways: (1) a 0–172.4 kPa (0–25 psia), 0–5 V pressure transducer (accurate to ±0.11%); (2) a dial pressure gauge; and (3) a standard pressure manifold. The pressure manifold, used in conjunction with a pressure release valve (Fig. 1) and the dial gauge, manually set the pressure level within the chamber. The pressure transducer monitored these pressures by way of a data acquisition board. Three K-type (chromium–aluminum) thermocouples with an accuracy of ±2% recorded temperature signals (Fig. 2).

EXPERIMENTAL RESULTS

A range of pressures was investigated to determine the effect of partial vacuums on the steady state drying rates for zero airflow. Before each test, the sample was saturated with water and ran through a 'spin' cycle to remove any excess free water. This procedure eliminated any variance between the starting masses of the samples, which were all approximately 52.0±0.25 g. Three tests were performed at 101.3 kPa (0″ Hg (vac.)), 82.7 kPa (5″ Hg (vac.)), 65.6 kPa (10″ Hg (vac.)) and 48.2 kPa (15″ Hg (vac.)). Only one test was taken at 41.4 kPa (20″ Hg (vac.)). The heater power was constant at 288 W for every test, resulting in a fixed heat flux ($\approx$5400 W m^{-2}) over the area of the cloth (0.05 m^2). Each sensor sampled at a rate of 0.5 Hz with a typical test on the order of 2700 s.

Figure 5 illustrates the results of a typical drying run. During each experiment, the cloth dried to approximately its 'bone dry' mass. Since the cloth sample completes each test within a prescribed range of starting and ending masses, a normalization function is used to develop dimensionless results. This formula is

$$m^* = \frac{V(t) - V(t = t_{\text{final}})}{V(t = t_0) - V(t = t_{\text{final}})}. \quad (1)$$

Equation (1) forces the ordinate to begin at unity and terminate at zero. The abscissa is normalized by dividing each time value by the final time of the slowest test. Thus the slowest run commences at $t^* = 0$ and ends at $t^* = 1$. Faster runs terminate at t^* values of

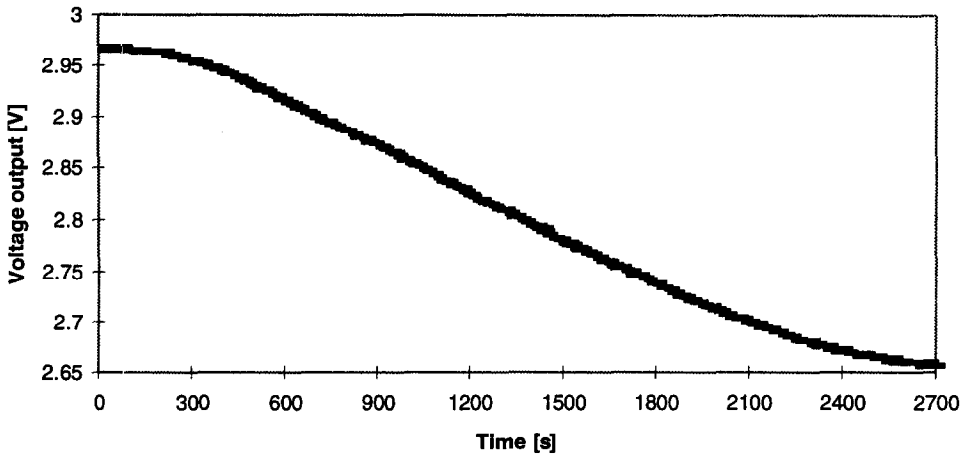

Fig. 5. Voltage vs time plot of a typical experimental run (run 14—atmospheric pressure).

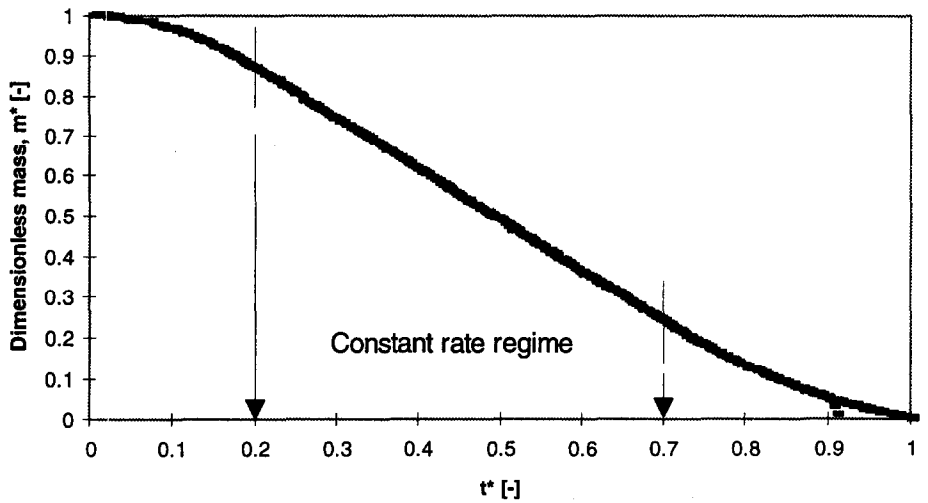

Fig. 6. Nondimensional mass plot of averaged atmospheric data (runs 14, 21, 22).

less than unity. Figure 6 depicts a normalized m^*–t^* curve.

Examination of Fig. 6 reveals the three distinctive drying regimes which are characteristic of a low-intensity drying process [12]. The linear range in Fig. 6 is approximately from $t^* = 0.2$–0.7. Outside this range the slope of the drying curve asymptotes to zero. A least-squares fit of the drying curve slope reveals a dimensionless drying rate.

Two different samples of the same material (cotton) were used for data. Figure 7 displays each normalized drying rate slope. The normalized drying rates are determined by dividing the individual drying rates by the atmospheric pressure drying rate. Consequently, the qualitative improvement in the drying rate produced by the two different samples are identifiable. Figure 7 indicates a definite improvement in drying rates due to a vacuum. The average slope increases in power-law fashion as pressure to the -0.5 power as pressure decreases. The maximum observed improvement is 62% at 39.52 kPa (0.39 atm).

THEORETICAL ANALYSIS

The majority of the fluid is removed during the constant rate regime (see Figs. 5 and 6). Therefore, this study will focus on the constant rate portion of the drying curve and attempt to predict mass transfer rates as a function of the ambient conditions. The analysis is similar to that of Ramadhyani [13].

A schematic for the static analysis is given in Fig. 8. The assumptions for the static analysis are:

(1) The evaporation process is laminar. As pressure decreases, the Rayleigh number decreases sharply and remains well below the turbulence limit of 10^9.

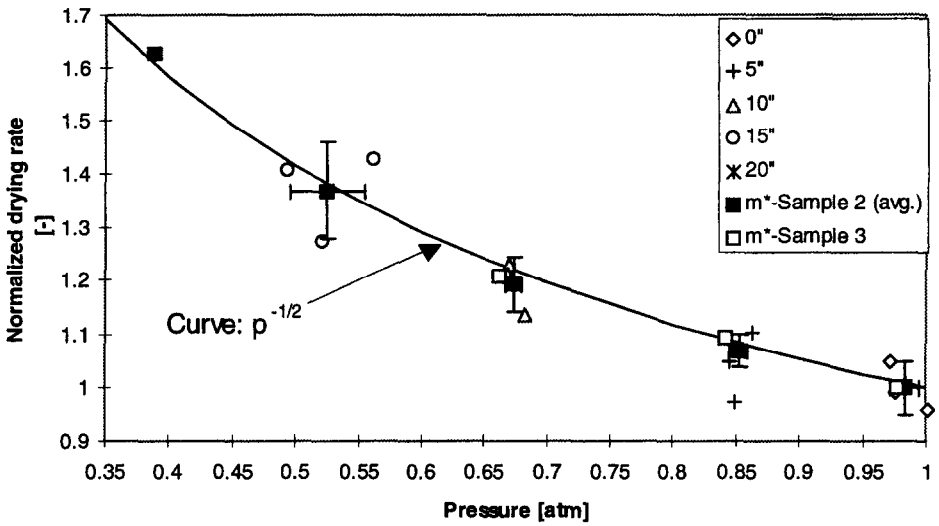

Fig. 7. Dimensionless drying rates vs pressure.

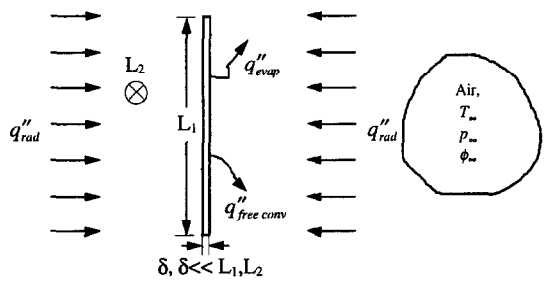

Fig. 8. Schematic of 'static' drying.

(2) The process is at steady-state with no internal heat generation.
(3) There are no potential or kinetic energy effects.
(4) Within each pressure level, the thermophysical properties of all fluids are constant at the film temperature $T_{film} = 0.5(T_\infty + T_{sat})$.
(5) Edge effects are neglected, as they are considered to be small compared with the area of the sample.
(6) The plate maintains a constant temperature, T_{sat}.
(7) Incident radiation from sources other than the two heaters is negligible.
(8) All surfaces behave as blackbodies, i.e. $\alpha = \varepsilon = 1.0$.

An energy balance yields

$$\dot{E}_{in} - \dot{E}_{out} + \dot{E}_{gen} = \dot{E}_{st}. \tag{2}$$

Applying (2) and the assumption gives

$$q''_{rad} - q''_{free\,conv} - q''_{evap} = 0. \tag{3}$$

Neglecting the free convection heat transfer, since it is small relative to the radiation heat transfer, (3) becomes

$$q''_{rad} = q''_{evap} = \dot{m}''_{evap} h_{fg}. \tag{4}$$

For this investigation, the radiation heat transfer rate is the input to the process. The evaporation mass transfer rate is a function of a mass transfer coefficient and a concentration difference. Specifically

$$\dot{m}''_{evap} = h_m(\rho_s - \rho_\infty) \tag{5}$$

and, therefore,

$$q''_{rad} = h_{fg} h_m(\rho_s - \rho_\infty). \tag{6}$$

Some of the terms in (6) may be simplified. The relative humidity ϕ_∞ is defined as

$$\phi_\infty = \left.\frac{\rho_\infty}{\rho_{sat}}\right|_{T_\infty, p_\infty}. \tag{7}$$

Substituting (7) into (6) gives

$$q''_{rad} = h_{fg} h_m(\rho_{sat}|_{T_s} - \phi_\infty \rho_{sat}|_{T_\infty}). \tag{8}$$

The density, ρ_s, was replaced by ρ_{sat} (at T_∞) owing to assumption (6). Equation (8) contains two unknowns, T_s and h_m. However, (8) may be further simplified by the fundamental thermodynamic relationship known as the Clausius–Clapeyron eqns [13, 14]. The Clausius–Clapeyron equation relates the latent heat of vaporization to pressure and volumetric data:

$$\frac{1}{p_{sat}} \frac{dp_{sat}}{dT} = \frac{h_{fg}}{RT^2}. \tag{9}$$

Equation (9) may now be integrated. The following integration assumes that h_{fg} is constant over the temperature range T_s to T_∞, thereby giving

$$\int_{p_{sat}(T_\infty)}^{p_{sat}(T_s)} \frac{dp_{sat}}{p_{sat}} = \int_{T_\infty}^{T_s} \frac{h_{fg}}{RT^2} dT \tag{10}$$

Table 2. Experimental results

Run	Average pressure [kPa (psia)]	Average temperature T_∞ [°C (°F)]	Initial mass [g]	Final mass [g]	Ambient pressure [kPa] (in. Hg)	Ambient relative humidity [%]
14	101.49 (14.72)	33.9 (93.1)	51.40	18.55	100.91 (29.80)	15.4
15	87.49 (12.69)	35.8 (96.5)	51.70	18.40	100.91 (29.80)	15.4
16	86.39 (12.53)	31.2 (88.1)	51.30	18.50	100.24 (29.60)	17.0
17	69.15 (10.03)	32.7 (90.9)	51.50	18.20	100.24 (29.60)	17.0
18	52.88 (7.67)	34.9 (94.9)	51.80	17.85	100.24 (29.60)	17.0
19	86.12 (12.49)	32.1 (89.7)	51.40	18.50	99.56 (29.40)	29.2
20	85.63 (12.42)	37.7 (99.8)	51.00	18.50	98.37 (29.05)	38.8
21	98.94 (14.35)	34.4 (94.0)	51.00	18.60	100.58 (29.70)	18.0
22	98.60 (14.30)	34.7 (94.4)	51.40	18.80	98.37 (29.05)	20.7
23	67.91 (9.85)	37.2 (99.0)	51.40	18.50	98.37 (29.05)	20.7
24	67.84 (9.84)	36.6 (97.9)	51.50	18.10	98.37 (29.05)	20.7
25	56.95 (8.26)	38.7 (101.6)	51.30	18.30	99.56 (29.40)	12.0
26	49.99 (7.25)	38.4 (101.1)	51.00	17.90	99.56 (29.40)	12.0
31	39.37 (5.71)	42.7 (108.8)	51.75	20.00	100.58 (29.70)	27.0

$$\ln p_{\text{sat}}\Big|_{p_{\text{sat}}(T_\infty)}^{p_{\text{sat}}(T_s)} = \frac{-h_{\text{fg}}}{RT}\Big|_{T_\infty}^{T_s} \tag{11}$$

$$\frac{p_{\text{sat}}|_{T_s}}{p_{\text{sat}}|_{T_\infty}} = \exp\left[\frac{h_{\text{fg}}}{R}\left(\frac{1}{T_\infty} - \frac{1}{T_s}\right)\right]. \tag{12}$$

Assuming that the water vapor can be approximated as an ideal gas gives

$$\frac{\rho_{\text{sat}}|_{T_s}}{\rho_{\text{sat}}|_{T_\infty}}\frac{T_s}{T_\infty} = \exp\left[\frac{h_{\text{fg}}}{R}\left(\frac{1}{T_\infty} - \frac{1}{T_s}\right)\right]. \tag{13}$$

Substituting (13) into (8) yields

$$q''_{\text{rad}} = h_m h_{\text{fg}}\left[\rho_{\text{sat}}\Big|_{T_\infty}\frac{T_\infty}{T_s}\exp\left\{\frac{h_{\text{fg}}}{R}\left(\frac{1}{T_\infty} - \frac{1}{T_s}\right)\right\} - \phi_\infty \rho_{\text{sat}}\Big|_{T_\infty}\right]. \tag{14}$$

Equation (14) contains two unknowns: T_s and h_m, where the relative humidity is constant. The radiant heat q''_{rad} is known as is the ambient temperature T_∞. The cloth surface is T_{sat} and corresponds to the ambient pressure level owing to assumption (6). The mass transfer coefficient h_m may be obtained from eqn (14) and used in eqn (5) to solve for the steady-state drying rate.

To verify the agreement of this analytical model with the experimental data, a comparison is developed in Table 2. Since the surface conditions and the liquid–solid bonding effects are unknown, the surface conditions were approximated using the saturation conditions of the total chamber pressure for the liquid state. Thus, at 99.7 kPa (0.984 atm), an ambient temperature of 307.50 K (93.83°F) and an ambient relative humidity of 18%, eqns (14) and (5) predict a drying rate of $15.21*10^{-3}$ g s^{-1}. The nondimensional, experimental drying rates for experiments 14, 21 and 22 (the atmospheric tests) were averaged and found to be 1.26. From Fig. 6 the constant rate regime is estimated to exist between $t^* = 0.7$ and 0.2. Taking the difference and multiplying by the normalization time 2700 s, the constant rate regime is approximately 1350 s in duration. Multiplying the nondimensional slope with the dimensionless time duration of the constant rate regime indicates that $1.26*0.5 = 0.63$ or 63% of the total amount of water in the sample was removed during this regime. Referring to Table 2, the average amount of water removed during the cycle for the atmospheric runs was 32.63 g. Sixty-three percent of the total, therefore, gives the approximate amount removed during the constant rate regime. This is $0.63*32.63 = 20.56$ g.

For the model, multiplying the calculated drying rate of $15.21*10^{-3}$ g s^{-1} drying rate with the estimated duration of the constant rate regime give $15.21*10^{-3}*1350 = 20.54$ g. This figure is in close agreement with the experimentally determined value.

Figure 9 compares the normalized drying rates predicted by eqn (14) to the experimental data. The drying rates compare favorably through 67.89 kPa (0.67 atm), but diverge at pressures below this point. Equation (14) does not take into account the absorption properties of the surface, in this case, cotton. The thermophysical properties used in (14) were those of liquid water at the total pressure, since surface temperature measurements were not included in the experimental tests.

In vacuum drying a completely external approach (effects of solid surface ignored) is thus only valid to approximately 70.93 kPa (0.7 atm) for cotton. Below this pressure the water/solid interaction effects must be taken into account. Above this pressure, eqn (14) predicts steady state drying rates accurately within 20% of measured data. Figure 7 indicates the maximum recorded drying slope is approximately 1.62 times greater than the atmospheric rate. Cotton is a hydrophilic solid, meaning it absorbs water into its

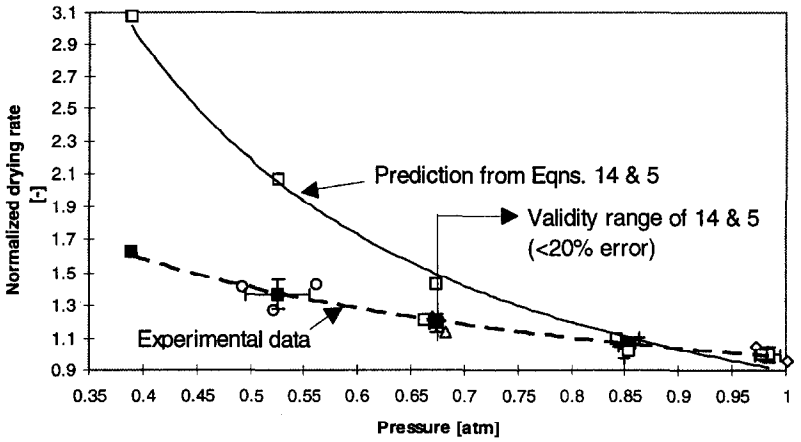

Fig. 9. Comparison of experimental results to drying rates predicted by eqns (14) and (5).

fiber structure. Chen and Pei [12] cited experimental data indicating that activation energy of bound water is different from the heat of vaporization of water due to the sorption characteristics of the material. Several authors have attempted to quantify this absorption effect, including Luikov [1]. Equation (14) also does not take into account the effects of capillaries, as water collects within these small tube-like structures. Lampinen [15] modified the chemical potential of water within the capillaries to account for a loss of vapor pressure inside the capillaries.

CONCLUSIONS

Introducing partial vacuum inside the drying chamber increased the steady-state drying rates by 62% over a range of pressures from atmospheric to 39.52 kPa (0.39 atm). The improvement in drying rates follows a pattern consistent with pressure to the -0.5 power.

This study also presents an analytical model for the steady state mass transfer coefficient for vacuum drying based on the assumption of fabric evaporating in the same manner as a free surface of water. Experimental data to verify eqn (14) agreed to within 20% for pressures above 67.89 kPa (0.67 atm). Below this pressure the improvement in the steady-state drying rate may be estimated by taking the inverse square root of the chamber pressure (in atmospheres).

Unfortunately, Fig. 7 does not indicate any preferred operating zone for vacuum assisted drying. As the pressure decreases, the drying rate increases in a power-law fashion (over the range of tests). The experimental and analytical results confirm that reducing pressure through 39.52 kPa (0.39 atm) has the effect of increasing the steady-state drying rate by as much as 62%.

Acknowledgement—The authors would like to thank the staff and support personnel at the Ray W. Herrick Laboratories at Purdue University for the usage of the facilities and their assistance.

REFERENCES

1. Luikov, A. V., *Heat and Mass Transfer in Capillary Porous Bodies*. Pergamon Press, London, 1966.
2. Åström, A., The influence of vacuum on the drying of paper. *Drying Technology*, 1988, **53**, 271–286.
3. Lehtinen, J. A., A new vacuum-drying method for paper, board and other permeable mats. In *Drying* '80, ed. A. S. Majumder. Hemisphere, New York, 1980, pp. 347–354.
4. Ahrens, F. and Journeaux, I., An experimental and analytical investigation of a thermally induced vacuum drying process for permeable mats. In *Drying* '84, ed. A. S. Majumder. Hemisphere, New York, 1984, pp. 281–291.
5. Forthuber, D. and McCarty, P., Drying heat sensitive and/or hazardous materials utilizing a fully continuous vacuum system. In *Drying* '84, ed. A. S. Majumder. Hemisphere, New York, 1984, pp. 380–385.
6. Smol'skiy, B. M., Fel'dman, R. I. and Gisina, K. B., Heat and mass transfer through an adsorbing layer in vacuum drying of heat-sensitive materials. *Heat Transfer—Soviet Research*, 1982, **14**, 75–81.
7. Harris, R. A. and Taras, M., Comparison of moisture content distribution, stress distribution, and shrinkage of red oak lumber dried by a radio-frequency/vacuum drying process and a conventional kiln. *Forest Products Journal*, 1984, **34**, 44–54.
8. Simpson, W. T., Vacuum drying northern red oak. *Forest Products Journal*, 1987, **37**, 35–38.
9. Malczewski, J. and Kaczmarek, W., Vacuum contact drying of seeds. *Drying Technology*, 1989, **7**, 59–69.
10. Wadsworth, J. I., Velupillai, L. and Verna, L. R., Microwave-vacuum drying of parboiled rice. *Trans. ASAE*, 1990, **33**, 199–210.
11. Shi, X. Q. and Maupoey, P., Vacuum osmotic dehydration of fruits. *Drying Technology*, 1993, **11**, 1429–1442.
12. Chen, P. and Pei, C. T., A mathematical model of drying processes. *International Journal of Heat and Mass Transfer*, 1989, **32**, 297–310.
13. Ramadhyani, S., Diffusion of heat and mass. Class notes, Purdue University, W. Lafayette, IN, 1994.
14. Wark, K., *Advanced Thermodynamics for Engineers*. McGraw-Hill, New York, 1995.
15. Lampinen, M. J., Mechanics and thermodynamics of drying: A summary. In *Drying* '80, ed. A. S. Majumder. Hemisphere, New York, 1980, pp. 11–16.